

Yamato 791197

Anorthositic regolith breccia
52.4 g



Figure 1: Yamato 791197 a feldspathic regolith breccia from the Yamato Mountains.

Introduction

Yamato 791197 (Fig. 1) was found on bare ice near the Yamato Mountains, by the JARE-20 meteorite search party in November, 1979 (Fig. 2 and 3). This 4.5 x 4.2 x 2.8 cm nearly complete stone was covered with a thick dusty gray fusion crust (Fig. 1, 17). Abundant, angular, white and gray clasts are set in a dark brown glassy matrix. Although initially it resembled a carbonaceous chondrite, examination of thin sections revealed a distinctive brecciated texture and the presence of numerous lithic and mineral fragments glass spherules and glassy patches in the matrix (Yanai and Kojima, 1984).

Petrography and Mineralogy

Yamato 791197 is a feldspathic regolith breccia containing a diversity of clasts types (Fig. 4), including troctolite (Fig. 5), dolerite (Fig. 6), norite, and anorthosite, and some with granulitic and cataclastic textures. Mineral fragments in the matrix include olivine, pyroxene, feldspar, and glassy spherules (Yanai and Kojima, 1984; Takeda et al., 1987; Ostertag et al., 1986; Takeda et al., 1986). Although most of the clasts and fragments are of highlands origin, there have been basaltic materials identified (Goodrich and Keil, 1986), which is also consistent with its intermediate composition (see below).

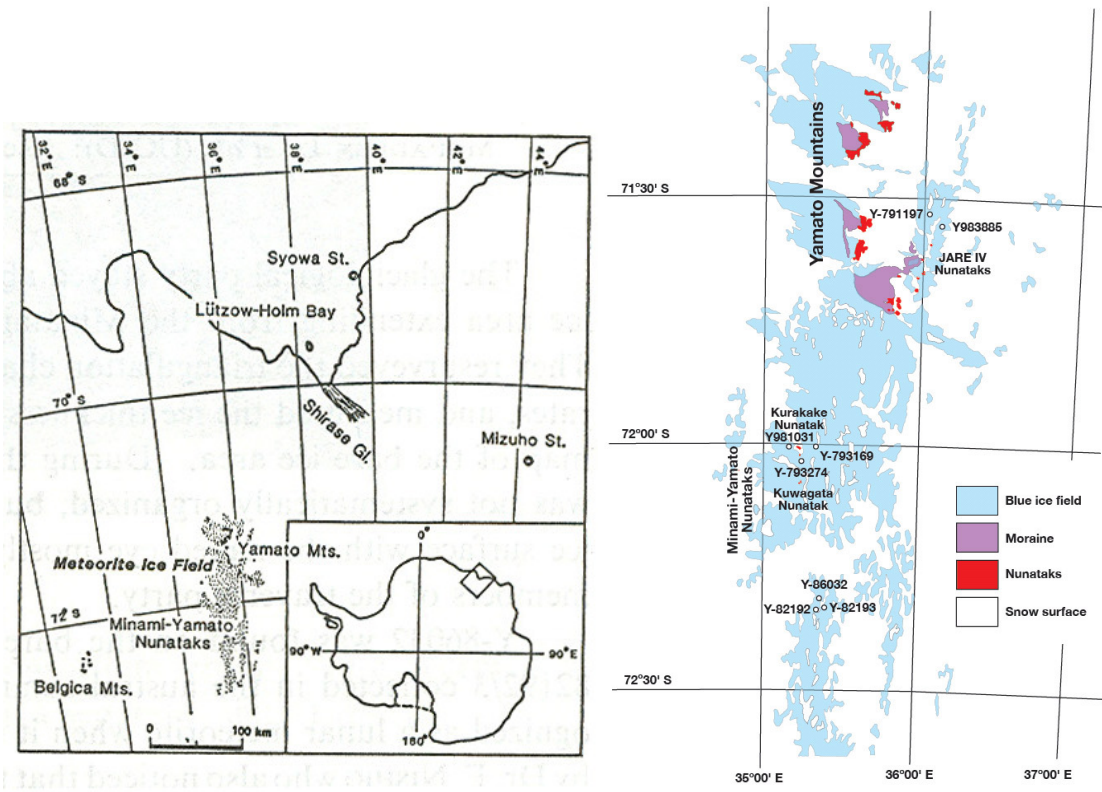


Figure 2: Location map for the Yamato Mountains. Figure 3: Detailed location map for the Yamato lunar meteorites (map courtesy of the NIPR). Y791197 is near the top of the map.

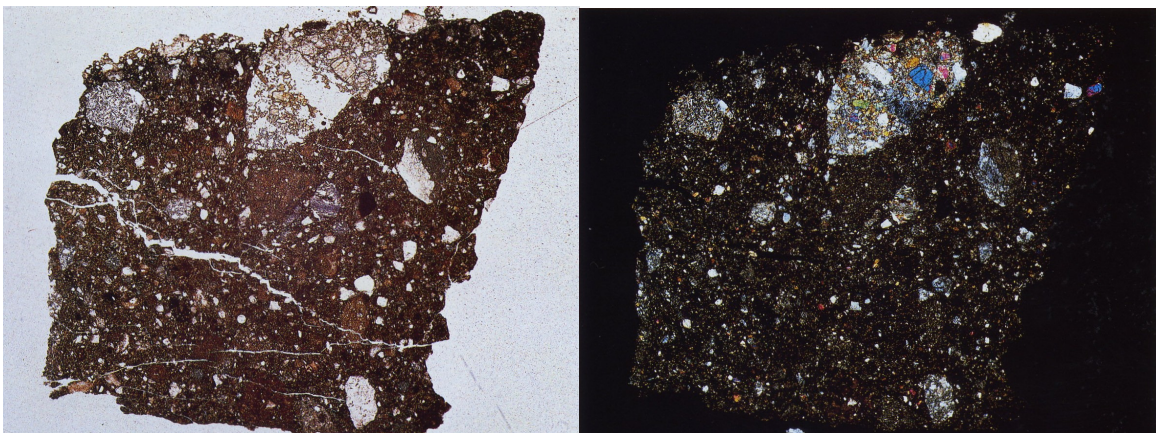


Figure 4: plane polarized light (left) and crossed polars (right) photomicrographs of Yamato 791197. Field of view is 2 mm (from Yanai and Kojima, 1984).



Figure 5 (left): crossed polarization photomicrograph of a troctolite clast from Yamato 791197. Figure 6 (right): crossed polarization photomicrograph of a dolerite clast from Yamato 791197. Both clasts are visible in the top center and left (respectively) of the thin section (from Yanai and Kojima, 1984).

As an example of the diversity of materials in Y-791197, the section studied by Ostertag et al. (1986) contains melt breccias, recrystallized lithic clasts and breccias, impact glass, fragmental breccias, and darker regolith breccias (Figure 7 and Table 1). The range of feldspars present in Y-791197 is narrow and calcic, from An₉₂ to An₉₈ (Fig 8). Olivines are largely Fo₅₀ to Fo₉₀, with a few more fayalitic (Fig. 8). And pyroxene compositional range is large in all sections examined including those by Yanai and Kojima (1984) and Takeda et al. (1987) (Figs. 8 and 9), and comparable to the range documented in Apollo feldspathic breccias (Fig. 9,10).

Table 1: Clast population in Yamato 791197 (section 73-2) from Ostertag et al. (1986).

Recrystallized lithologies	65.4
Granulitic breccias	10.4
Granulitic anorthosites	6.1
Cataclastic anorthosites	13.7
Polymict fragmental breccia	12.8
Feldspathic fragmental breccia	12.4
Crystalline melt breccias	16.6
Vitric or devitrified glasses	7.0
Fragmental breccias	12.6
Lithic fragments	0.4
Mineral fragments	8.1
Total	100.1

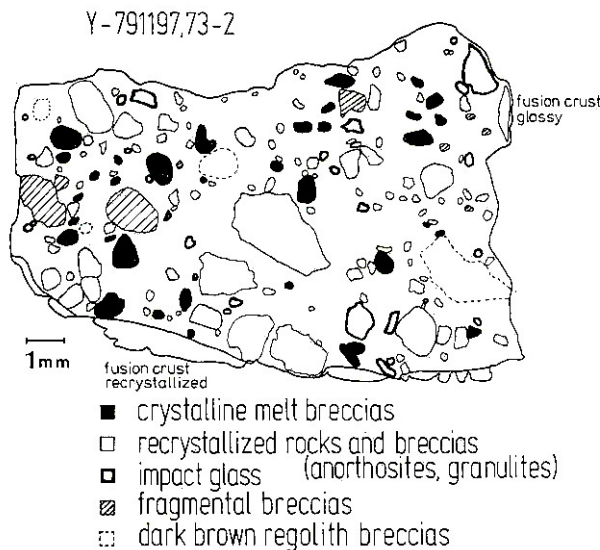


Figure 7: Sketch of primary components of section 73-2 of Yamato 791197, described by Ostertag et al. (1986).

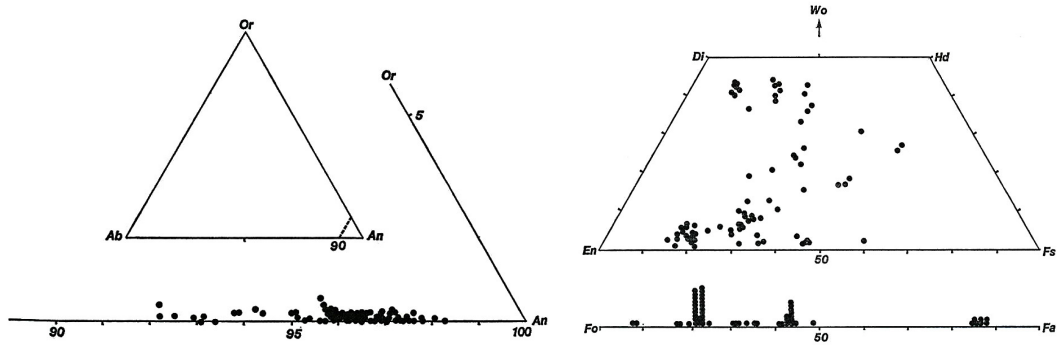


Figure 8: Compositional range of plagioclase, olivine, and pyroxene in Y-791197 (from Yanai and Kojima, 1984).

Chemistry

The feldspathic nature of Yamato 791197 is also reflected in its bulk compositional features. It is Al-rich with analyses ranging from 25 to 28 wt% Al_2O_3 (Table 2). Its FeO, MgO and CaO contents also fall within highlands groupings (Korotev, 2005), making it of clear highlands origin. However, it does fall at the low end of the range of Al_2O_3 contents and the high end of Mg# for highlands meteorites, making its chemistry somewhat distinct from the others. It is most similar in composition to ALH A81005, both in terms of its REE contents (Fig. 11), and other lithophile incompatible elements (Fig. 12). The levels of REE are lower than other highland materials and even the average highlands REE contents (Fig. 11), reflecting derivation from a KREEP-free

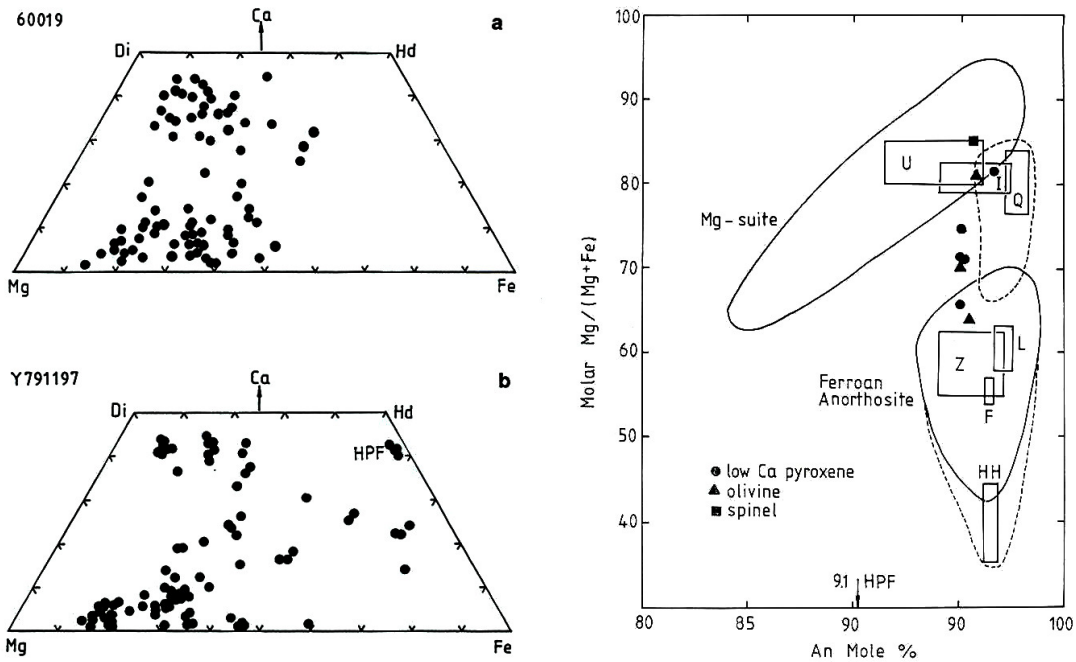


Figure 9 (left): Comparison of Yamato 791197 pyroxene compositions with those from an Apollo 16 feldspathic regolith breccia (from Takeda et al., 1987).

Figure 10 (right): Compositions of ferromagnesian minerals and plagioclase feldspar from clasts found in Y-791197, compared to fields of the Mg-suite, ferroan anorthosites, and lettered clasts from ALH81005 (Treiman and Drake, 1983). The compositional range between Mg-suite and FAN fields is rare in Apollo samples, but relatively common in lunar meteorite samples (Korotev (2005).

source (e.g., Ostertag et al., 1986; Warren and Kallemeyn, 1986; Lindstrom et al., 1986). Enrichment of many of the labile, volatile trace elements (e.g., Cd, Te, Zn, Sb) is thought to be due to the effects of volcanic exhalations, because the levels measured in Yamato 791197 are higher than ALH A81005, but similar to levels measured in Apollo 16 samples known to be affected by exhalations (Fig. 13; Kaczaral et al., 1986). Finally, concentrations of the siderophile elements Ni, Au and Ir, in Y-791197 are high and chondritic relative, indicating that they have been set by meteoritic contamination that is common in lunar regolith samples (Fig. 14; Ostertag et al., 1986).

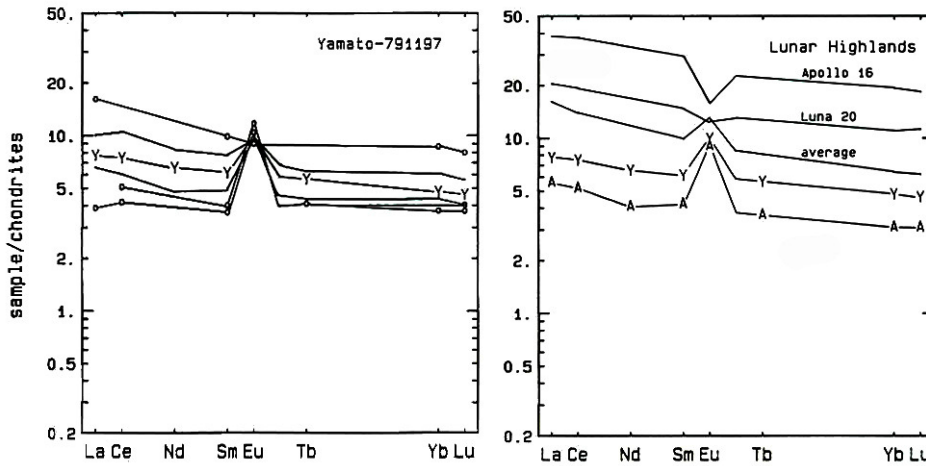


Figure 11: Rare earth element patterns for individual clasts and weighted average for Yamato 791197 samples (Lindstrom et al., 1986).

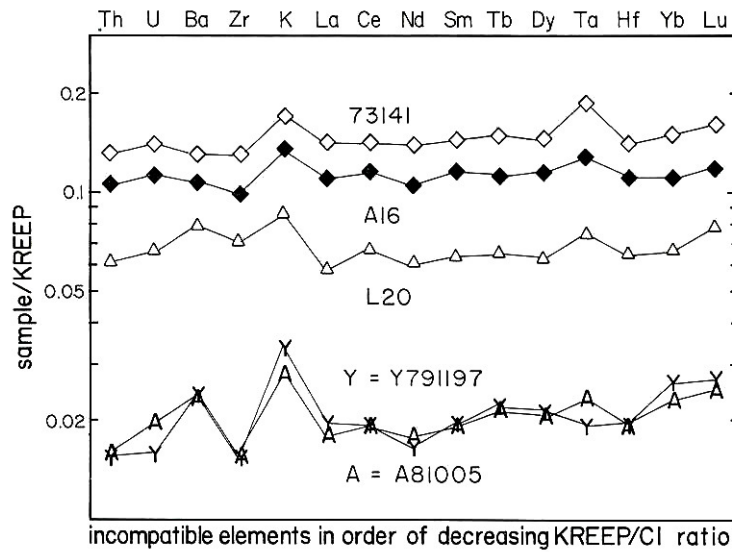


Figure 12: Incompatible element diagram for Yamato 791197, normalized to KREEP values, and compared to ALH A81005, and Apollo and Luna highland samples (from Warren and Kallemeyn, 1986).

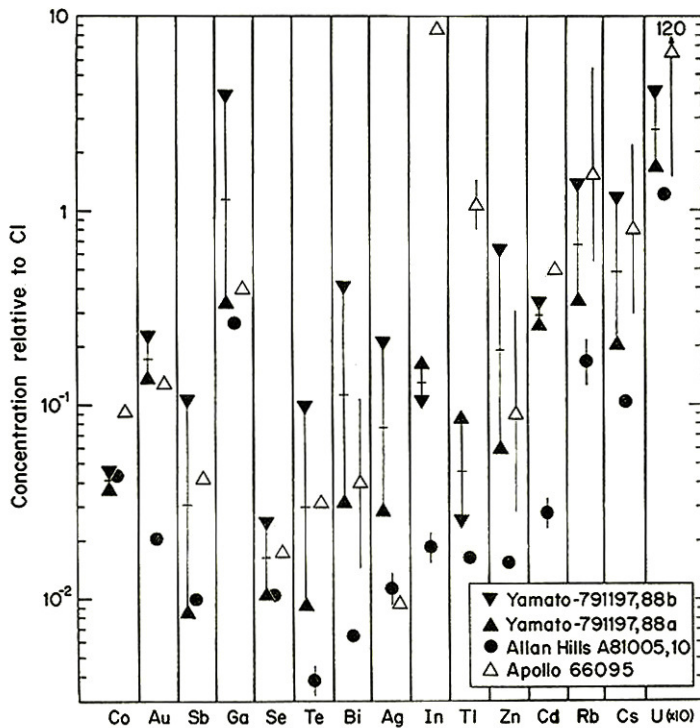


Figure 13: Volatile elements measured in two splits of Yamato 791197 and compared to the lunar meteorite ALH A81005 and an Apollo anorthositic gabbro that has been enriched by lunar volcanic exhalations (from Kaczaral et al., 1986).

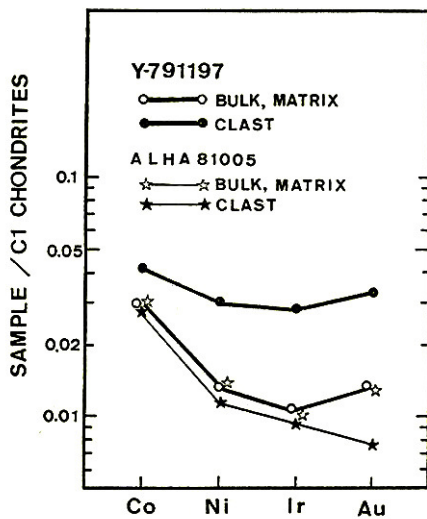


Figure 14: Siderophile element concentrations in a clast and bulk sample of Yamato 791197 compared to the same from ALH A81005 (from Ostertag et al., 1986).

Radiogenic age dating

A plagioclase-rich clast from Yamato 791197 was separated and prepared for ^{40}Ar - ^{39}Ar analysis, and yielded an age of 4.065 (± 0.093) Ga (Kaneoka and Takaoka, 1986; Fig. 15). Several studies of the Rb-Sr system led to uncertain results, perhaps due to analysis of materials of a mixture of sources and ages (Takahashi et al., 1986; Nakamura et al., 1986), but did conform to the initial Sr isotopic ratio lower than BABI and high $^{207}\text{Pb}/^{204}\text{Pb}$ and $^{206}\text{Pb}/^{204}\text{Pb}$, both of which are lunar properties. Additional work by Takahashi and Masuda (1987) showed that the age of Y-791197 is 3.95 (± 0.24) Ga, consistent with the

Ar-Ar age (Fig. 16). Whether these ages are primary, or were reset by a late heavy bombardment, is not clear.

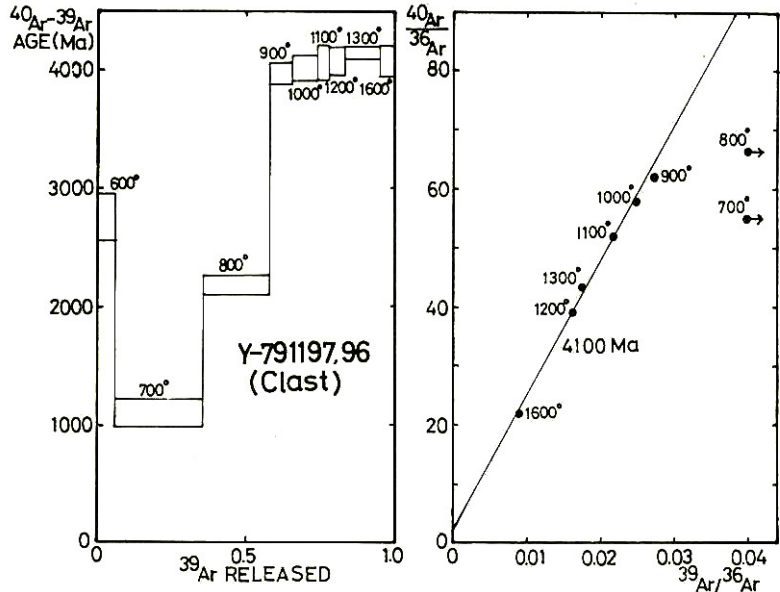


Figure 15: ^{40}Ar - ^{39}Ar plateau age and release history for a feldspathic clast from Yamato 791197 (Kaneoka and Takaoka, 1986).

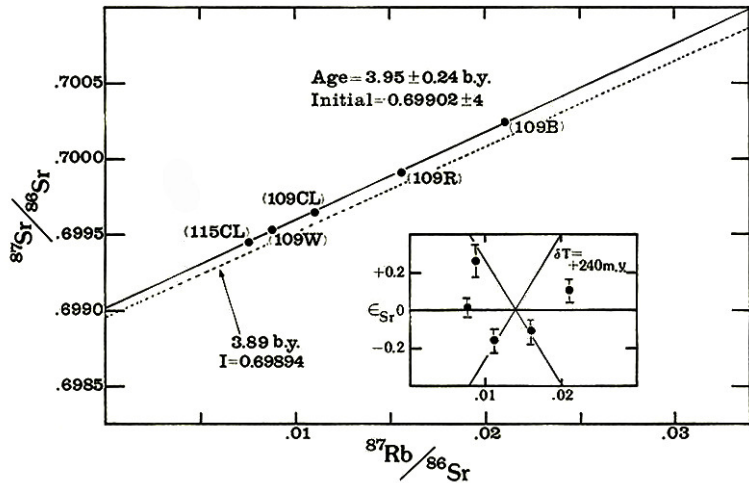


Figure 16: ^{87}Sr - ^{86}Sr vs. ^{87}Rb - ^{86}Sr isochron diagram for feldspathic clasts from Yamato 791197 (Takahashi and Masuda, 1987).

Cosmogenic isotopes and exposure ages

Noble gas contents of Yamato 791197 are intermediate, indicating origin from a moderately mature regolith. Measurements of Eugster et al. (1986) result in a 910 Ma residence time in the lunar regolith. Mn, Ca, Al, Cl and Be isotopic studies show a very short Moon-Earth transfer time ($\ll 0.1$ Ma; Nishiizumi et al., 1991a), in agreement with the cosmic ray tracks (Sutton, 1986) and measurements of Takaoka (1986). Nishiizumi et al. (1991a) also determine a very short terrestrial age (0.03 to 0.09 Ma). Thus an ejection age is constrained to 0.03 to 0.19 Ma (Lorenzetti et al., 2005). These results all indicate a very young ejection age, and very short transfer time from the Moon to the Earth.

Table 1a. Chemical composition of Yamato 791197

<i>reference</i>	1	2	3	4	4	4	4	5	5	6	6	7	7	8	8	
<i>weight</i>		59.3	197	36.35	21.62	30.34	8.22	71	19	21.4	23.2	11.69	52.6	41.6	8	
<i>method</i>	c	e	e	e	e	e	e	f	f	e	e	e	e	e	e	
SiO ₂ %	43.14															44.9
TiO ₂	0.35	0.367	0.284							0.3	0.32					0.4
Al ₂ O ₃	26.01	25.12	26.63							27.7	26					27.3
FeO	7.03	6.497	5.699	5.98	6.06	6.27	5.99			6.7	6.8	6.561	6.394	5.51		5.71
MnO	0.08	0.093	0.084							0.087	0.084	0.082	0.086			0.12
MgO	6.22	7.048	5.97							5.8	7.7					5.76
CaO	15.33	15.95	15.11	15	15.1	14.9	14.8			15.3	15.5			15.65		15.86
Na ₂ O	0.33	0.325	0.315	0.324	0.334	0.331	0.331			0.34	0.32	0.337	0.337	0.325		0.3
K ₂ O	0.02	0.035	0.028	0.025	0.027	0.023	0.023			0.028	0.026	0.029	0.029	<0.15		0.028
P ₂ O ₅	0.31	0.023														0.02
S %	0.41															
<i>sum</i>																
Sc ppm		16.5	12.5	12.87	13.78	14.02	12.82			13.5	12.7	12.6	12	11.7		
V		39	30							30	24					
Cr	889.5	1034	880	940	933	938	906			855.3	780	930	880	865		753
Co		16.9	18.4	21.6	17.1	19.4	19.2	18.2	21.2	19.8	"173"	26.2	24.2	5.51		
Ni		100	154	214	152	185	193			170	"1940"	214	220	151		
Cu																
Zn		50	21					18	189							
Ga		9.87	3.2					3.16	37.4				3.3			
Ge																
As												<0.5	0.37	<0.2		
Se								0.193	0.457			0.83	0.5			
Rb								0.68	2.66			<10	8	<4		
Sr		118	140	148	152	149	141			130	150	100	171	150		
Y																
Zr			26	47	47	42	40			30	35	35	35	30		
Nb																
Mo																
Ru																
Rh																
Pd ppb																
Ag ppb								6.1	43.9							
Cd ppb								170	220							
In ppb								13	8.4							
Sn ppb																
Sb ppb								1.4	17.2				<100	<30		
Te ppb								21.3	228							
Cs ppm			0.059					0.037	0.216			<0.1	0.08	<0.12		
Ba		34	29	30	32	36	38			40	38	30	30	26		
La		3.24	2.16	2.24	2.95	2.55	2.59			2.16	2.06	2.17	2.51	1.93		
Ce		8.76	5	5.7	7.4	6.6	6.7			5.6	5.2	4	4.65	5.18		

Pr													
Nd	5.24	3	3.6	4.7	4.3	3.6			3.5	3.2	3.5	3.6	3
Sm	1.56	0.96	1.11	1.44	1.25	1.24			1.08	1.01	1.23	1.15	0.975
Eu	0.723	0.72	0.75	0.791	0.77	0.762			0.8	0.76	0.704	0.72	0.734
Gd									1.3	1.3	1.65	1.6	
Tb	0.33	0.216	0.26	0.33	0.29	0.3			0.26	0.21	0.28	0.22	0.227
Dy	2.22	1.4							1.6	1.45	1.96	1.6	
Ho	0.48	0.28											
Er	.												
Tm	0.23								0.16	0.16	0.2	0.15	
Yb	1.34	0.95	0.97	1.17	1.08	1.03			1.12	0.95	1.05	1.12	0.896
Lu	0.19	0.135	0.143	0.174	0.159	0.155			0.17	0.14	0.159	0.138	0.127
Hf	1.11	0.73	0.85	1.03	0.93	0.93			0.78	0.85	0.92	1.33	0.73
Ta	0.16	0.078	0.103	0.128	0.107	0.108			0.1	0.12	0.2	0.1	0.099
W ppb													<800
Re ppb													
Os ppb													
Ir ppb	5.9	6.4	9.7	4.5	6.6	4			6	6.6	6.3	6.8	5.5
Pt ppb													
Au ppb	1.3	<2	1.8	1.4	3.4	4.2	18.6	30.7	2.5	"37"	3.6	7.3	1.5
Th ppm	0.43	0.28	0.31	0.36	0.33	0.29			0.39	0.29	0.34	0.34	0.291
U ppm	0.14	0.079	0.1	0.13	0.12	0.13			0.1	0.09		0.1	0.09

technique (a) ICP-AES, (b) ICP-MS, (c) wet chemistry (d) FB-EMPA, (e) INAA, (f) RNAA, (g) XRF

Table 1b. Light and/or volatile elements for Yamato 791197

Li ppm													
Be													
C													
S													
F ppm													
Cl													
Br		0.16	0.15	0.27	0.18	0.46					<0.1	<0.08	
I													
Pb ppm													
Hg ppb													
Tl									12	3.5			
Bi									3.5	45			

1) Yanai and Kojima (1984); 2) Ostertag et al. (1986); 3) Warren and Kallemeyn (1986); 4) Lindstrom et al.(1986); 5) Kaczarek et al.(1986); 6) Fukuoka et al.(1986); 7) Koeberl (1988); 8) Korotev et al. (2003).

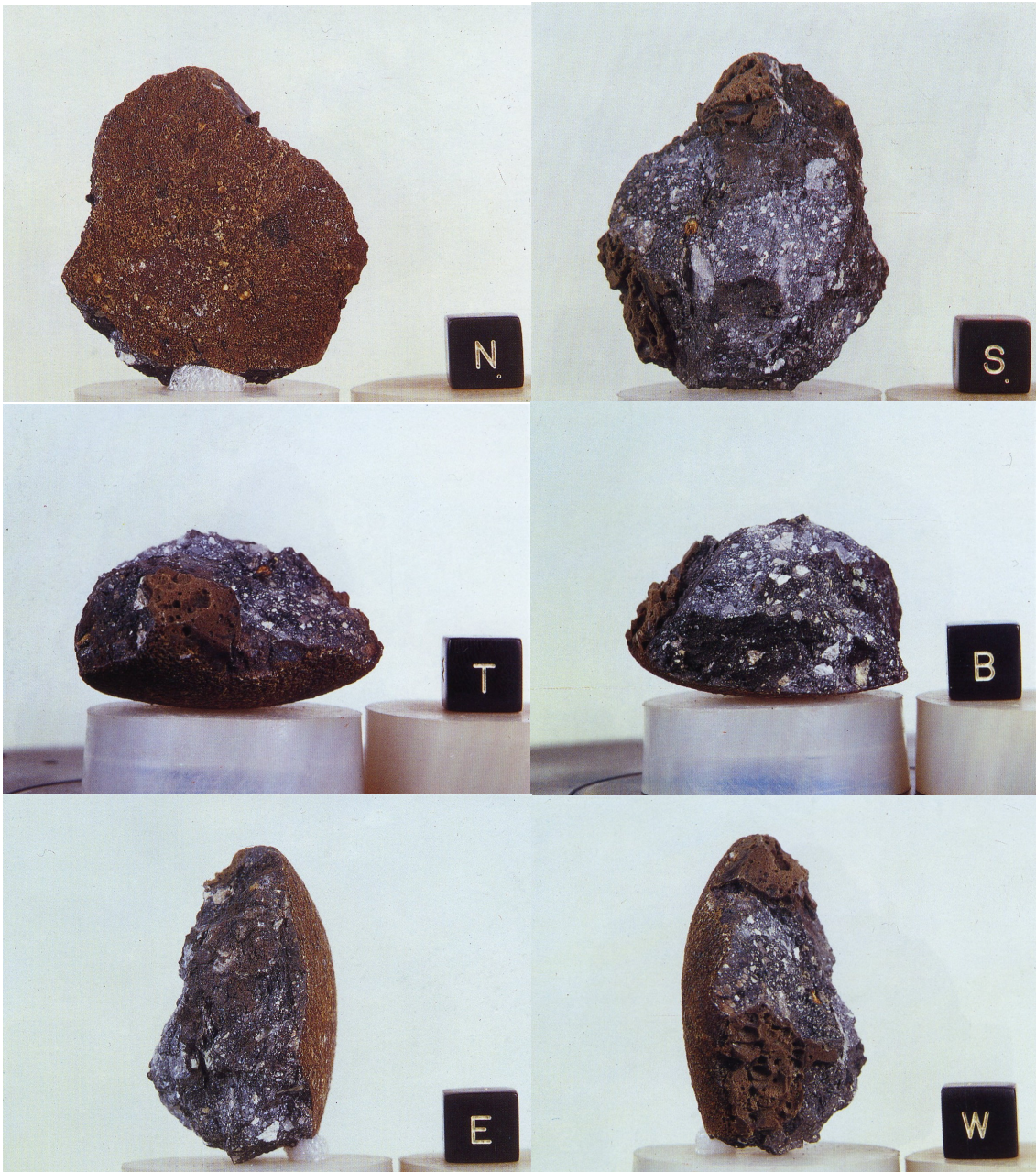


Figure 17: Six different views of Yamato 791197.

K. Righter – Lunar Meteorite Compendium - 2010